D6 facilitates cellular migration and fluid flow to lymph nodes by suppressing lymphatic congestion

*Kit Ming Lee,[1] *Clive S. McKimmie,[1] Derek S. Gilchrist,[1] Kenneth J. Pallas,[1] Robert J. Nibbs,[1] Paul Garside,[1] Victoria McDonald,[2] Christopher Jenkins,[3] Richard Ransohoff,[4] LiPing Liu,[4] Simon Milling,[1] Vuk Cerovic,[1] and Gerard J. Graham[1]

[1]Division of Immunology, Infection and Inflammation, Glasgow Biomedical Research Centre, University of Glasgow, Glasgow, United Kingdom; [2]Mater Medical Research Institute, South Brisbane, Australia; [3]Sir William Dunn School of Pathology, University of Oxford, Oxford, United Kingdom; and [4]Neuroinflammation Research Center, Lerner Research Institute, Cleveland, OH

Lymphatic endothelial cells are important for efficient flow of antigen-bearing fluid and antigen-presenting cells (APCs) from peripheral sites to lymph nodes (LNs). APC movement to LNs is dependent on the constitutive chemokine receptor CCR7, although how conflicting inflammatory and constitutive chemokine cues are integrated at lymphatic surfaces during this process is not understood. Here we reveal a previously unrecognized aspect of the regulation of this process. The D6 chemokine-scavenging receptor, which is expressed on lymphatic endothelial cells (LECs), maintains lymphatic surfaces free of inflammatory CC-chemokines and minimizes interaction of inflammatory leukocytes with these surfaces. D6 does not alter the level of CCR7 ligands on LECs, thus ensuring selective presentation of homeostatic chemokines for interaction with CCR7$^+$ APCs. Accordingly, in D6-deficient mice, inflammatory CC-chemokine adherence to LECs results in inappropriate perilymphatic accumulation of inflammatory leukocytes at peripheral inflamed sites and draining LNs. This results in lymphatic congestion and impaired movement of APCs, and fluid, from inflamed sites to LNs. We propose that D6, by suppressing inflammatory chemokine binding to lymphatic surfaces, and thereby preventing inappropriate inflammatory leukocyte adherence, is a key regulator of lymphatic function and a novel, and indispensable, contributor to the integration of innate and adaptive immune responses. (*Blood*. 2011;118(23): 6220-6229)

Introduction

Lymphatic endothelium plays essential roles in regulating fluid and chemokine-dependent antigen-presenting cell (APC) movement from peripheral sites to draining lymph nodes (LNs).[1] The chemokine family[2] is functionally subdivided into inflammatory and constitutive subsets.[3] Inflammatory chemokines are involved in recruiting leukocytes to sites of infection or damage, whereas constitutive chemokines are involved in more precise, tissue-specific, trafficking, including movement into secondary lymphoid organs as part of the adaptive immune response. Initiation of adaptive immune responses requires selective migration of APCs expressing the constitutive chemokine receptor, CCR7, to LNs.[4] To facilitate this, lymphatic endothelium selectively expresses, and presents, the CCR7 ligands CCL19 and CCL21. However, in the context of inflamed peripheral tissues, in which inflammatory chemokines will be abundant, it is unclear how selective presentation of constitutive chemokines by lymphatic endothelium is achieved.

In addition to the family of signaling chemokine receptors, we and others have been studying a subfamily of atypical chemokine receptors characterized by an apparent inability to signal after ligand binding.[5,6] Further studies have shown some of these receptors to be active as chemokine-scavenging receptors, implicating them in negative regulation of chemokine-driven processes.[7-9] We are particularly interested in the D6 chemokine-scavenging receptor.[10] This molecule scavenges by binding inflammatory CC-chemokines with high affinity, internalizing them, and targeting them for intracellular degradation. D6 does not bind, or alter cellular responses to, constitutive CC-chemokines, such as CCL19 or CCL21, or chemokines belonging to any other subfamily and is therefore specific for inflammatory CC-chemokines.[5,10-12] In D6-deficient mice, exaggerated inflammatory responses have been observed, in all tissues in which D6 is normally expressed,[5,13-18] indicating its importance for resolution of in vivo inflammatory responses. However, the major site of D6 expression in vivo is on lymphatic endothelial cells (LECs),[19] and it is difficult to argue for a major role for these cells in inflammatory chemokine scavenging.[20] In addition, D6 is expressed on some leukocyte subtypes,[17,21] including macrophages[19] but predominantly on B cells and dendritic cells (DCs), which are not cells that are typically attracted to, and able to scavenge chemokines at, the epicenter of inflammatory responses. Thus, the cellular basis for in vivo D6 function is currently unclear. In particular, the roles for D6 on LECs have remained elusive.

Here we have focused specifically on roles for D6 on lymphatic endothelium and its importance for fluid and cellular trafficking from peripheral tissues to LNs. We report that D6 plays an essential function in regulating lymph flow and cellular efflux from inflamed peripheral sites to draining LNs. D6 achieves this role by preventing

Submitted March 22, 2011; accepted September 16, 2011. Prepublished online as *Blood* First Edition paper, October 6, 2011; DOI 10.1182/blood-2011-03-344044.

*K.M.L. and C.S.M. contributed equally to this study.

The online version of this article contains a data supplement.

The publication costs of this article were defrayed in part by page charge payment. Therefore, and solely to indicate this fact, this article is hereby marked "advertisement" in accordance with 18 USC section 1734.

association of inflammatory CC-chemokines with lymphatic surfaces, thus blocking interactions between inflammatory leukocytes and lymphatic vessels. Accordingly, in D6-deficient mice, inappropriate inflammatory leukocyte accumulation around, and within, lymphatic vessels "congests" the lymphatic system, impairing fluid and cellular movement (including APCs) from peripheral sites to LNs. These data therefore reveal a novel aspect of the regulation of lymphatic function and identify lymphatic endothelial–expressed D6 as an essential coordinator of innate and adaptive immune responses.

Methods

Mice

D6-deficient[14,22] and WT mice were maintained on C57Bl/6 (lipopolysaccharide [LPS] injection studies) or FVB/N (skin inflammation studies) backgrounds. Experiments were approved by the University of Glasgow ethical review committee.

Antibodies

Antibodies include biotin-conjugated Gr-1, FITC/PE-conjugated CD11b, goat anti–mouse Lyve-1, and biotin-conjugated anti–mouse CCL2 antibodies (R&D Systems); AlexFlour(AF)647-conjugated streptavidin, Qdot565-conjugated goat anti–FITC antibody, and AF488-conjugated anti–goat polyclonal antibody (Invitrogen); isotype controls, FITC-conjugated anti–mouse CD3e, PE-conjugated anti–mouse CD19, biotin/allophycocyanin/FITC/PE-conjugated anti–mouse CD11b, FITC-conjugated anti–mouse Gr-1, FITC-conjugated anti–mouse Ly6C, and PE-conjugated anti–mouse Ly6G antibodies (BD Biosciences). For CCL2 detection, the tyramide signal-amplification kit (PerkinElmer Life and Analytical Sciences) was used with modifications to the manufacturer's protocol. Biotinyl tyramide was diluted 1:70 in amplification reagent, and sections incubated for 3 minutes. Streptavidin-PE (eBioscience) diluted 1:280 was used as a secondary detection reagent.

Induction of cutaneous inflammation

Mice were treated with 12-O-tetradecanoylphorbol 13-acetate (TPA) as described.[14,22] C57Bl/6 mice received 200 μL of 200μM TPA to shaved dorsal skin, and FVB/N mice received 150 μL of 50μM TPA. For LPS-induced inflammation, mice were injected subcutaneously in the footpad with either 1 μg of ultra-pure LPS (Calbiochem) in 50 μL sterile PBS or PBS alone. At appropriate times, mice were killed and popliteal LNs collected.

Fluorescence images were acquired using Zeiss Image examiner on an LSM-510 confocal microscope (Carl Zeiss), except where stated in the figure legends.

LNs and lymph cells, collected as described,[23] were analyzed by flow cytometry on a FACSCalibur (BD Biosciences) or MACSQuant (Miltenyi). Up to 30 000 (LNs) or 2×10^5 cells (lymph) were acquired. For analysis of Langerhans cells (LCs), LNs were digested using liberase-3 (Roche Applied Science) and stained for CD11c (BD Biosciences) and EpCAM/CD326 (BioLegend).

For measurement of CCR2 on myelomonocytic cells, suspensions of popliteal LNs from D6-deficient mice were incubated in complete RPMI/20mM HEPES and 30 ng/ml AF647-labeled hCCL2 (Almac Sciences) at 37°C for 30 minutes in the presence or absence of a 10× molar excess of unlabeled CCL2 as described.[21] The cells were then washed and CCL2 binding measured by flow cytometry. Cells left unstained were used as a control for background fluorescence.

Generation of subcutaneous air pouches

Dorsal skin air pouches were generated as described[24] and injected with a mixture of recombinant human CCL3-L1 (which, in contrast to hCCL3, is a high-affinity murine D6 ligand[25]) and CXCL8 (R&D Systems) in PBS/0.1% BSA or PBS/0.1% BSA alone. One hour later, inguinal LNs were collected and homogenized, on ice, in 200 μL ice-cold PBS with protease inhibitors (Sigma-P8340; Sigma Aldrich). The protein concentration was measured using a protein assay kit (Pierce Chemical). A total of 50 μL of LN lysate was used for measurement of hCCL3-L1 and hCXCL8 using sandwich ELISA kits (R&D Systems).

AF647-labeled hCCL5 or AF647-CXCL8 (2 μg; Almac Sciences) was injected into air pouches. Inguinal LNs draining the air pouches were processed for frozen sectioning and analyzed using an LSM510 confocal microscope (Carl Zeiss).

Assessment of tissue fluid content

Edema was assessed by injecting mice intravenously with AF750-conjugated BSA (AF750-BSA; Invitrogen) and lymphatic drainage from skins to LNs, by subcutaneous injection of AF750-BSA. Imaging was used to measure dye retention within the skin and data analyzed using Living Image Version 4.0 software (IVIS Spectrum; Caliper Life Sciences). Twelve to 15 points of transillumination targeting the injected site were selected for 3-dimensional volumetric measurement of retained AF750-BSA. Mice were exposed to transilluminated light for 1 second with excitation at 710 nm and emission from AF750-BSA collected at 780 nm with a cooled-CCD camera. Binning was set at medium with F/Stop at 4.0. Subcutaneous injection of Evans blue dye was used to assess fluid movement into LNs. LNs were soaked for 24 hours in formamide to extract dye, centrifuged (16 000*g*) to remove tissue debris, and dye content of the supernatant determined at OD 620 nm.

Langerhans cell trafficking assay

Mice were TPA-painted to inflame skin for 24 hours. Immediately after a further TPA paint, skin was painted with FITC (5 mg/mL in 1:1 acetone/dibutylphthalate, Sigma-Aldrich).[26] LNs were removed and frozen for microscopy, or digested, and analyzed by flow cytometry.

Adoptive transfer of labeled DCs to inflamed skin

Bone marrow-derived DCs[27] were stained with CFSE or 5(6)-carboxy tetramethylrhodamine (TAMRA).[28] CFSE and TAMRA-stained cells were washed, mixed 1:1, and injected subcutaneously into TPA-inflamed skin. After 24 hours, inguinal LNs were removed and 8-mm skin biopsies taken, frozen, and 8-μm sections cut for immunostaining. LNs were digested using Liberase-3 (Roche Applied Sciences), and cells were analyzed by flow cytometry to quantify fluorescently stained leukocytes.

HUVEC THP-1 binding assay

HUVECs maintained in EndoGRO-VEGF Complete-Media Kit (Millipore) were transfected with D6GFP, or control vectors, using TransPass HUVEC-Transfection Reagent (New England Biolabs). Twenty-four hours after transfection, cells were placed in fresh medium containing 10 ng/mL mouse TNF (R&D Systems) for 24 hours and 2×10^5 TAMRA-labeled (Invitrogen) THP-1 cells added and allowed to adhere for 1 hour. After this, cells were gently washed with PBS and dissociated using trypsin. The number of bound THP-1 cells was quantified by flow cytometry.

Microscopy and image acquisition

Images were gathered using either (1) an LSM 510 confocal microscope (Carl Zeiss; Figures 1B-C, 4B-D, and 6A) and AIM LSM 510 Version 3.2 software or (2) an Apotome Imager.Zl fitted with an AxioCam MRm digital camera (Carl Zeiss; Figures 4D-E and 5B) with Axiovision Version 4.7.2 software. All acquired images were individually exported and saved as JPEG or TIFF files prior to embedding in PowerPoint (note that all Apotome images were saved as TIFFs). Figures 1Bi and 4C were subsequently cropped using Axiovision Version 4.8.1 software and Figures 4D-E and 5B were cropped usingAdobe Photoshop Elements Version 6.0. The imaging medium used for mounting was Vectashield with DAPI (Vector Laboratories) for all figures with the exception of Figures 1C and

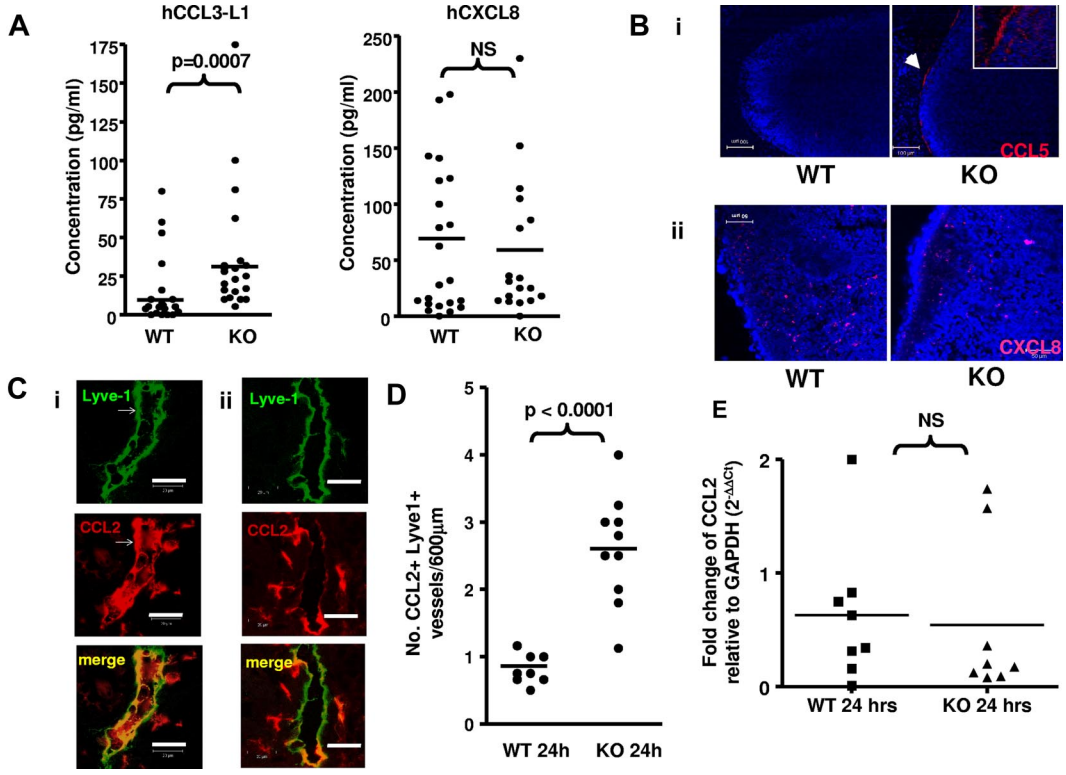

Figure 1. D6 prevents association of inflammatory chemokines with LN endothelial cells. (A) ELISA measurements of hCCL3-L1 and hCXCL8 in inguinal LNs 1 hour after injection into subcutaneously air pouches of WT and D6-deficient mice. LNs were homogenized, on ice in 200 μL PBS and cellular debris pelleted before ELISA measurement using the supernatant. NS indicates not significant. (Bi) Two representative confocal images illustrating the association of AF647-CCL5 (injected into subcutaneously air pouches) with the subcapsular sinus of inguinal LNs in D6-deficient (KO), but not WT, mice. An arrow indicates the sites of AF647-CCL5 positivity (shown as a cropped image in the inset). Original magnifications ×20 with a scan zoom at 0.7 on a Plan-Neofcuar 20×/0.5 Ph2 objective. 4,6-Diamidino-2-phenylindole (DAPI, blue) was used as a nuclear stain for cells in the LN. Scale bar represents 100 μm. (Bii) Two representative confocal images demonstrating the lack of CXCL8 accumulation in the subcapsular sinus of WT or D6-deficient (KO) LNs. Original magnifications ×40 with a scan zoom at 0.7 on a Plan-Neofcuar 60×/1.3 oil objective. Scale bar represents 50 μm. (C) Frozen skin sections were stained with anti–mouse Lyve-1 monoclonal antibody (green) and anti–mouse CCL2 polyclonal antibody (red). Representative confocal images showing a CCL2-containing dermal lymphatic in inflamed skin of (i) a D6-deficient and (ii) a WT mouse 24 hours after TPA painting. Images were acquired at 63× magnification with a scan zoom at 1.7 on a Plan Apochromat 63×/1.4 oil Ph3 objective. Scale bar represents 20 μm. (D) The frequency of $CCL2^+$ lymphatics in the dermis of inflamed WT and D6-deficient skin per 600 μm of each section. (E) Relative CCL2 transcript levels in the skins of WT and D6-deficient mice 24 hours after TPA administration. PCR used the following primer sets: GAPDH forward, 5′-TGAACGGGAAGCTCACTGGC-3′; reverse, 5′-TCCACCACCCTGTTGCTGTAG-3′; CCL2 forward, 5′-TGAGTAGGCTGGAGAGC-TACA-3′; reverse, 5′-TCACTGTC- ACACTGGTCACTC-3′. PCR was performed as described previously.[21] Data are from > 3 (A-B) and 2 (C-E) independent experiments with n > 3 mice per experimental group for each individual experiment.

4C in which the imaging medium was Polyvinyl alcohol with DABCO (I,4-diazabicyclo[2.2.2]octane; Sigma-Aldrich).

Statistical analysis

Data were analyzed using Prism Version 3 software and used Student *t* test or Mann-Whitney, depending on the nature of the data distribution. Results are presented as mean ± SEM.

Results

D6 suppresses inflammatory CC-chemokine interactions with lymphatic endothelium

It has been proposed that lymphatic endothelial D6 blocks chemokine access from peripheral sites to lymph and LNs. However, analysis of the chemokine content of pseudo-afferent lymph from colitic rats[29] revealed high levels of CCL2 (160-375 pg/mL) and CCL5 (54-148 pg/mL). Thus, in WT animals, D6 does not block inflammatory CC-chemokine entry to lymph. To investigate whether lymphatic D6 regulates chemokine movement from lymph into LNs, we compared the movement of inflammatory CC-chemokines from peripheral tissues to draining LNs in WT and D6-deficient mice. This was done by injecting human (h) chemokines (to distinguish from murine chemokines) into subcutaneously air pouches and measuring their levels, in LNs, 1 hour later. We injected hCCL3-L1 (which binds murine D6 with high affinity[25]) and hCXCL8, which is not a D6 ligand[5,10-12] and which should be unaffected by the presence, or absence, of D6 in the mice. The results showed (Figure 1A) a modest, but significant, increase in hCCL3-L1 in D6-deficient, compared with WT, draining inguinal LNs. In contrast, no differences were seen in hCXCL8 levels in draining LNs. Notably, concentrations of both human chemokines were extremely low and, given that 10 μg of each was injected into the air pouch, represented, at best, very limited accumulation of the chemokines in LNs. This suggests that chemokines draining from inflamed sites are able to enter, and travel through, lymph without accumulating substantially in LNs.

To investigate the basis for the modest increase in hCCL3-L1 in more detail and to distinguish lymph-borne from LEC-produced inflammatory chemokines, we injected AF647-CCL5 (an alternative D6 ligand[12] as AF-hCCL3-L1 is not currently available) into subcutaneous air pouches and, 45 minutes later, examined its distribution in WT and D6-deficient inguinal LNs. As shown in Figure 1Bi, although AF647-CCL5 was undetectable in WT LNs, in D6-deficient mice it was found localized to the outer aspects of LNs, in a region corresponding to the walls of the subcapsular

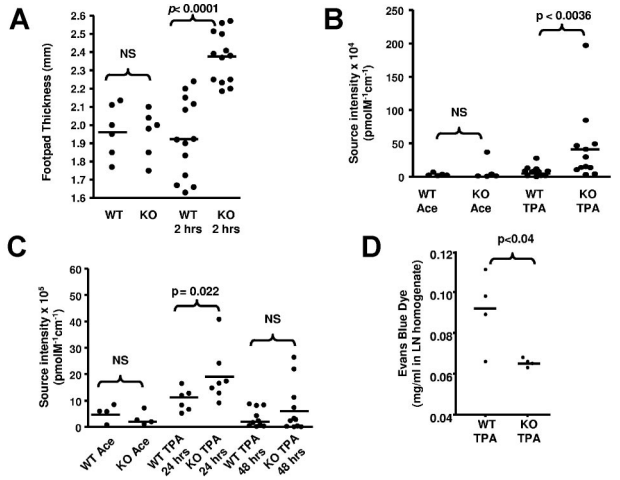

Figure 2. D6-deficient skin demonstrates impaired lymphatic function. (A) Inflamed D6-deficient footpads are thicker than inflamed WT footpads. Footpad thickness was measured 2 hours after subcutaneous injection of LPS, on H&E-stained sections of mouse paws at 5× magnification on a light microscope (Carl Zeiss) equipped with Axiovision Version 4.6, 12-2006 software. Measurement was done using the Axiovision Interactive Measurement analysis module (Carl Zeiss). (B) TPA-inflamed D6-deficient skin is more edematous than inflamed WT skin. Edema was measured by intravital imaging of dermal accumulation of intravenously injected AF750-BSA. WT Ace and KO Ace are acetone control treated mice. (C) Fluid drainage from TPA-inflamed skin is impaired in D6-deficient, compared with WT, mice as measured by clearance of subcutaneously injected AF750-BSA (see "Assignment of tissue fluid control"). WT Ace and KO Ace are acetone control treated mice. (D) LN drainage of subcutaneously injected Evans blue dye is impaired in TPA-inflamed D6-deficient, but not WT, mice. Evans blue dye was injected subcutaneously, LNs collected 1 hour later, and Evans blue dye accumulation in the LNs measured as described. (A-C) Data are from more than 3 independent experiments with $n > 3$ mice per experimental group for each individual experiment. (D) Results are from a single experiment.

sinus. This distribution is more clearly seen in the cropped image inset in Figure 1Bi. Importantly, although there was no subcapsular accumulation of the non-D6 binding fluorescent-CXCL8 (Figure 1Bii), it was detectable at equivalent levels in intra-LN sites in D6-deficient and WT mice. It is probable that significant LN hCCL3-L1 differences were not seen in Figure 1A as there is relatively little subcapsular sinus wall-associated chemokine and the extraction protocol is unlikely to have released surface-adherent chemokines.

In addition to LNs, when lymphatic vessels in inflamed skins of D6-deficient, but not WT, mice were investigated, they were seen to be strongly $CCL2^+$ (Figure 1C) with significantly more $CCL2^+$ lymphatic vessels in inflamed D6-deficient skin than in inflamed WT skin (Figure 1D). This is despite similar CCL2 transcript levels (Figure 1E), indicating that this difference results from enhanced deposition of CCL2 on lymphatic vessels in D6-deficient mice.

Therefore, D6 does not block entry of inflammatory CC-chemokines to lymph but prevents their association with lymphatic endothelium at inflamed peripheral sites and in the subcapsular sinus region of LNs.

D6 deficiency is associated with impaired lymphatic function

Next, we examined the impact of D6 deletion on lymphatic function. Whereas uninflamed D6-deficient, and WT, skins show no differences in thickness, inflamed D6-deficient skin is more edematous, and swollen, than inflamed WT skin as revealed by increased footpad-thickness after LPS injection (Figure 2A) and by increased retention of intravenously injected AF750-BSA after TPA painting (Figure 2B). To test whether the edema resulted from increased vascular leakage or impaired drainage, we injected AF750-BSA subcutaneously, which confirmed (Figure 2C) that direct movement of fluid from inflamed skin to LNs was impaired in D6-deficient, but not WT, mice, for up to 24 hours after AF750-BSA injection. This was also reflected in reduced accumulation of subcutaneously injected Evans blue dye in D6-deficient, compared with WT, LNs 30 minutes after injection into inflamed skin (Figure 2D). Notably (supplemental Figure 3C, available on the *Blood* Web site; see the Supplemental Materials link at the top of the online article), impaired drainage was also seen in D6-deficient mice as early as 30 minutes after AF750-BSA injection. These early differences suggest that this effect cannot be accounted for by differences in APC ingestion, and transfer of dye to LNs, as APC accumulation is not seen in LNs until 24 hours after cutaneous antigen administration.[30] Thus, D6-deficient mice display impaired lymphatic function.

D6 deficiency is associated with altered LN cellularity

Next, we examined draining LNs to gain insights into the basis for the impaired lymphatic function in inflamed D6-deficient mice. WT and D6-deficient inguinal LNs in uninflamed mice are of similar size (Figure 3A). However, 24 hours after TPA-application to dorsal skin, both WT and D6-deficient draining LNs increased in weight. Notably, and in agreement with a previous report,[16] the weight increase in D6-deficient mice was significantly greater than that in WT mice and correlated with a significant increase in LN cellularity (Figure 3B). Significant increases in popliteal LN cellularity of D6-deficient, compared with WT, mice were also

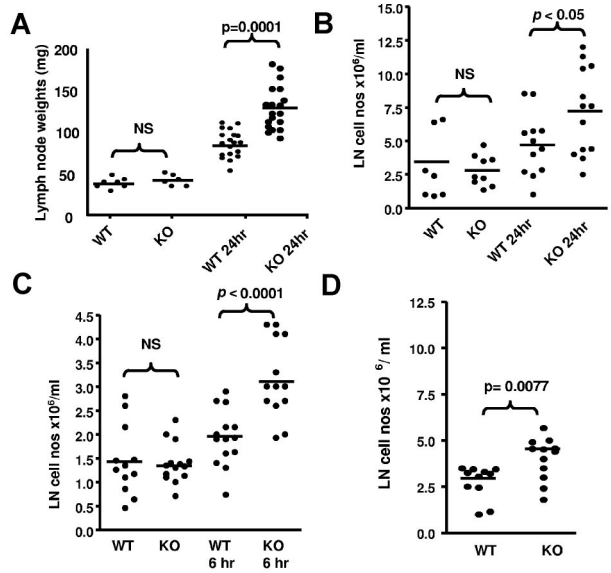

Figure 3. LN alterations in D6-deficient mice. (A) TPA painting leads to increased weight of D6-deficient inguinal LNs compared with WT inguinal LNs. These data were obtained by removing, and weighing, inguinal LNs from mice at rest and 24 hours after TPA painting. LNs were weighed on a ExplorerPro microbalance. (B) This weight increase is associated with an increase in D6-deficient LN cellularity. LNs were collected and dispersed into 1 mL of medium with DNAse and the cells counted on a hemocytometer. These data were obtained using WT and D6-deficient inguinal LNs collected at rest and 24 hours after TPA painting. (C) Footpad injection of LPS also increases LN cell numbers in D6-deficient, compared with WT, mice. These data are from popliteal LNs collected at rest (contralateral LNs draining PBS injected footpads), and 6 hours after LPS injection, and processed as in panel A. (D) Chemokine injection alone led to exaggerated increases in the cellularity of D6-deficient LNs. hCCL3 in PBS/0.1% BSA was injected into subcutaneously air pouches on the back of D6-deficient, or WT, mice and the cellular content of inguinal LNs, processed as in panel B, assessed 1 hour later. (A-D) Data are from 3 independent experiments with $n > 3$ mice per experimental group for each individual experiment.

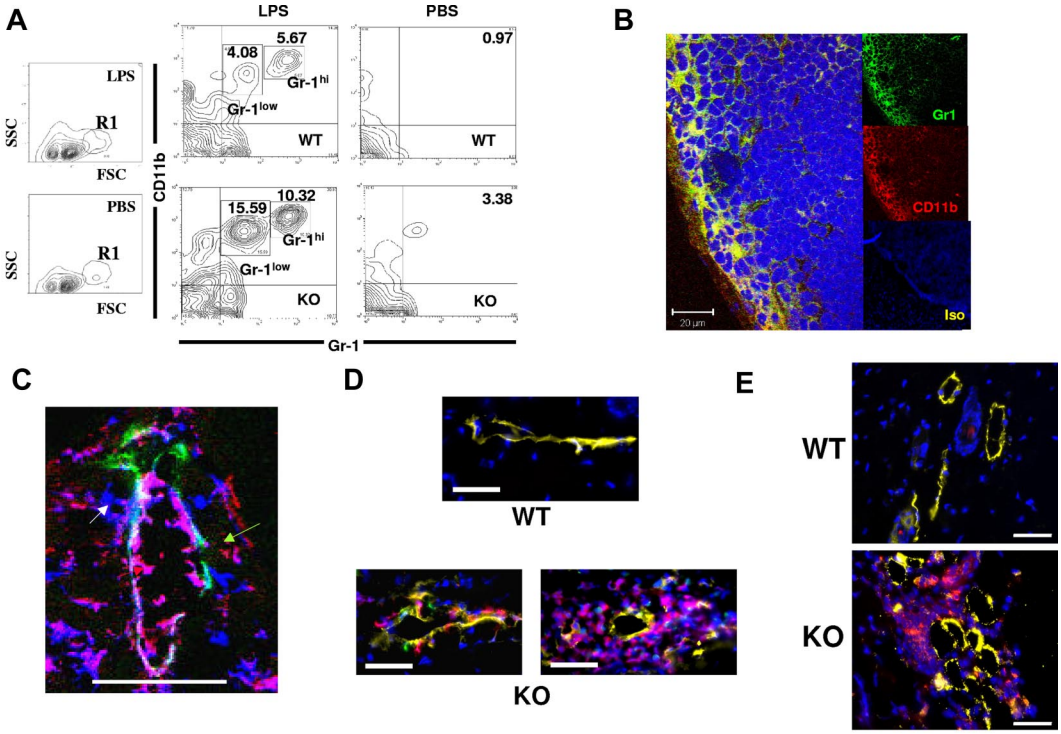

Figure 4. Perilymphatic myelomonocytic cell accumulation in D6-deficient mice. (A) Footpad injection of LPS leads to alterations in CD11b^{+}Gr1^{low} and CD11b^{+}Gr1^{hi} myelomonocytic cells in D6-deficient popliteal LNs. Representative FACS plots illustrating the R1 gate displaying the main increase in LN cell populations in LPS-treated, compared with PBS treated mice (first 2 panels). The remaining 4 panels show CD11b/Gr1 differences between WT (top) and D6-deficient (bottom) mice 24 hours after footpad injection of LPS, or control injection of PBS into the contralateral footpad. Numbers in the contour plots represent the percentage of the marked populations in each gate. Note that the 3.38% population in the D6-deficient, PBS, top right-hand quadrant, is not seen in other experiments and therefore does not represent a consistent cellular population in these mice. (B) Popliteal LNs from D6-deficient mice at 2 hours after LPS footpad injection were stained using anti–mouse Gr1 (green) and anti–mouse CD11b (red) monoclonal antibodies. In this representative confocal image, the CD11b^{+}Gr1^{+} cells are denoted in yellow (merge). DAPI (blue) was used for nuclear staining. The isotype control staining is shown in the lower of the 3 insets (Iso). Note that both the anti–Gr1 and anti–CD11b antibodies are of the same isotype (rat IgG2b kappa), and so only one isotype control was needed. Images were acquired at ×63 magnification with a scan zoom at 1.0 on a Plan-Apochromat 63×/1.1 oil Ph3 objective. Scale bar represents 20 μm. (C) A dermal lymphatic vessel stained for Lyve 1 (green), CD11b (red), and Gr1 (blue). Separate CD1b^{+} (green arrow), Gr1^{+} (white arrow), and CD11b^{+}Gr1^{+} (red arrow) cells are marked. Scale bar represents 50 μm. This image was cropped from a single confocal image, taken on a Zeiss LSM 510 confocal microscope. Original images were acquired at ×63 magnification with a scan zoom at 0.7 on a plan-apochromat 63×/1.4 oil Ph3 objective. (D) Perilymphatic accumulation of DCs in D6-deficient but not WT mice. DCs are labeled with CFSE/green (WT) or TAMRA/red (D6-deficient), and lymphatic vessels stained with Lyve1 (yellow). Nuclei are stained with DAPI (blue). Images were acquired using AxioVision Version 4.6, 12-2006 software on an Apotome fluorescence microscope (Zeiss AxioImager). Images were acquired at Xho magnification on an achroplan 1.0×/0.8w (water) objective. Scale bar represents 20 μm. (E) Mice were inoculated with MOG/CFA and skin examined by microscopy after 3 days. Sections from WT and D6-deficient mouse skins, at the site of inoculation, were stained for CD11c (red), Lyve-1 (yellow), and with DAPI (blue) staining for nuclei. Images were acquired using AxioVision software on an Apotome fluorescence microscope (Zeiss AxioImager). Images were acquired at Xho magnification on an achroplan 1.0×/0.8w (water) objective. Scale bar represents 50 μm. (A-B) Representative of at least 3 replicate experiments. (C-E) Representative of at least 2 replicate experiments. A minimum of 5 mice were used per experimental group for each of the experiments represented in this figure.

apparent after LPS injection into footpads (Figure 3C). Furthermore, chemokines alone were able to trigger increased inguinal LN cellularity in D6-deficient, compared with WT, mice as early as 1 hour after subcutaneous injection of the inflammatory chemokine CCL3 (Figure 3D).

Thus, D6 deficiency is associated with chemokine deposition on lymphatic surfaces, impaired lymphatic function and rapid, aberrant, cellular accumulation in LNs draining inflamed sites.

Myelomonocytic cells accumulate at perilymphatic sites in D6-deficient LNs

To identify the cellular basis for the differences reported in Figure 3, we analyzed the cellularity of WT, and D6-deficient, popliteal LNs after LPS footpad injection. T- and B-cell numbers increased proportionately in both WT and D6-deficient LNs, and no difference in LN architecture was observed (data not shown). However, differences were noted in a minor population (1%-2% of total LN cells) of FSChiSSClo cells (R1 in Figure 4A), which became more abundant in D6-deficient, compared with WT, LNs after LPS-induced inflammation. Further examination demonstrated that R1 contained a CD11b^{+} subpopulation, which increased to a greater extent in D6-deficient, compared with WT, LNs with major (Figure 4A) and significant (supplemental Figure 1A) increases specifically in the percentage of CD11b^{+}Gr1^{+} cells, including discrete Gr1^{hi} and Gr1^{low} populations. Increases in this population were also seen in D6-deficient, compared with WT, inguinal LNs draining TPA-inflamed skin, suggesting this to be a general consequence of inflammation (supplemental Figure 1B). These cells were also F4/80^{+} and predominantly Ly6C^{+} (data not shown) and will be referred to as myelomonocytic cells. Notably, although the LN weight increase in inflamed D6-deficient mice (Figure 3) is disproportionate to the increase in size of this minor cellular population, this is consistent with previous reports of modest DC accumulation precipitating large increases in overall LN cellularity.[31]

The myelomonocytic cells accumulated rapidly in D6-deficient LNs, with significant numbers being detected 2 hours after LPS application (supplemental Figure 1C-D), at which time they were barely present in WT LNs. Confocal microscopy of D6-deficient LNs revealed, again as early as 2 hours, that the myelomonocytic

cells were predominantly localized to the outer area of LNs in a region corresponding to the subcapsular sinus (Figure 4B) coincident with the distribution of immobilized chemokines (Figure 1B). Lower-resolution images (supplemental Figure 1E) indicated that, in contrast to their peripheral location in D6-deficient LNs, these cells were diffusely distributed in WT LNs. The rapid accumulation of myelomonocytic cells at the periphery of D6-deficient LNs prompted us to examine lymph as their possible source; and, indeed, flow cytometry (supplemental Figure 1F) revealed similar $CD11b^+Gr1^{low}$/$CD11b^+Gr1^{hi}$ populations in lymph. It should be noted that pseudo-afferent lymph is collected from the thoracic duct, and it is probable that higher numbers of these cells will be present in afferent lymph but removed after passage through LNs.[32] Together with the low magnification images in supplemental Figure 1E, this suggests lymph, and not blood, to be the major source of these cells.

Thus, impaired lymphatic function in D6-deficient mice is associated with rapid perilymphatic accumulation of chemokines and lymph-borne myelomonocytic cells in the subcapsular sinus region of LNs draining inflamed tissues.

Perilymphatic inflammatory leukocyte accumulation is also seen at inflamed peripheral sites in D6-deficient mice

Investigation of $Lyve1^+$ lymphatic vessels, in inflamed D6-deficient skin, revealed perilymphatic (but not periblood vessel, data not shown) cellular accumulation reminiscent of that seen in LNs. Specifically, inflammatory leukocytes, including $Gr1^+$, $CD11b^+$, and $CD11b^+Gr1^+$ cells, were closely associated with dermal lymphatic vessels in inflamed D6-deficient, but not WT, mouse skin (Figure 4C; supplemental Figure 2). The cells were associated with both subluminal and luminal aspects of lymphatic vessels; and, in keeping with their presence in lymph (supplemental Figure 1F), the $CD11b^+Gr1^+$ cells were predominantly luminally associated. In contrast (supplemental Figure 2), few $CD11b^+$ or $Gr1^+$ cells were seen associated with luminal or subluminal aspects of WT lymphatic vessels. To demonstrate that this perilymphatic cellular accumulation was not a consequence of enhanced chemokine levels in D6-deficient inflamed skin, we examined WT and D6-deficient skins 16 hours after TPA administration, at which time they show no significant differences in chemokine levels.[14] Perilymphatic inflammatory leukocyte accumulation was evident in inflamed D6-deficient dermis surrounding, and also attached to the lumenal face of, lymphatic vessels (supplemental Figure 3A). This accumulation is not seen in resting D6-deficient, or inflamed WT, skin. Enumeration of lymphatic vessels with associated $CD11b^+Gr1^+$ cells further demonstrated preferential association of these cells with inflamed D6-deficient, and not inflamed WT, lymphatic vessels at 16 hours (supplemental Figure 3B). Again (supplemental Figure 3C), inflamed D6-deficient skin was significantly more edematous than inflamed WT skin at this time point, indicating impaired lymphatic drainage.

To further examine the aberrant association of inflammatory cells with dermal lymphatics in inflamed D6-deficient mice, we dye-labeled bone marrow–derived DCs (BMDCs) and subcutaneously injected them into previously inflamed WT or D6-deficient mice. Twenty-four hours later, although no BMDCs were associated with dermal lymphatics in WT mice, in D6-deficient mice numerous BMDCs were seen lining lymphatic vessels and, in some cases, large clusters of such cells were evident (Figure 4D). Lower-magnification images (supplemental Figure 3D) indicated that DCs are not clustered in regions distant from D6-deficient lymphatics, indicating their specific association with vessels. This confirms the aberrant association of inflammatory leukocytes with D6-deficient lymphatic vessels in inflamed peripheral tissues and, together with the 16-hour data, demonstrates that this is not simply a consequence of enhanced chemokine levels in inflamed D6-deficient skin.

We have reported reduced responses of D6-deficient mice in the experimental autoimmune encephalomyelitis model of multiple sclerosis[33], in which D6-deficient mice displayed dermal aggregates of DCs. We now show that, similar to Figure 4D, whereas $CD11c^+$ cells are not associated with lymphatic vessels in WT skin after subcutaneous myelin oligodendlocyte glycoprotein/complete freund's adjuvant (MOG/CFA) administration, perilymphatic aggregates of $CD11c^+$ cells are seen in similarly treated D6-deficient mice (Figure 4E). Lower-magnification images show DC aggregation specifically in the vicinity of lymphatic vessels (supplemental Figure 3E). This demonstrates that inappropriate perilymphatic accumulation of inflammatory leukocytes is also seen in inflamed D6-deficient mice in models of autoimmune inflammatory pathologies.[33] Thus, perilymphatic accumulation of inflammatory leukocytes, coincident with the CCL2 deposition in Figure 1C, is seen at peripheral inflamed sites.

D6 deficiency is associated with impaired APC trafficking from inflamed sites

A possible consequence of the findings in Figure 4 is that APC migration from D6-deficient skin to draining LNs will be compromised under inflamed conditions. To test this, we compared migration of FITC-labeled LCs (defined as $EpCAM^+$)[34] and dermal migratory DCs ($CD11c^+$I-A/I-E^{hi})[35] from inflamed WT and D6-deficient skin to inguinal LNs. There were no differences in LC or resident DC ($CD11c^+$I-A/I-E^{int})[35] numbers in LNs from uninflamed WT or D6-deficient mice (supplemental Figure 4A). Inflammation was induced in dorsal skin using TPA; and, 24 hours later, FITC was applied to the skin and accumulation of $FITC^+$ LCs, and migratory DCs, assessed in draining LNs 24 hours later. There was significantly reduced accumulation of $FITC^+$ LCs in D6-deficient, compared with WT, LNs, indicating impaired LC migration in inflamed D6-deficient mice (Figure 5A-B; supplemental Figure 4B). In addition (Figure 5C), LCs reaching LNs in D6-deficient mice were significantly more "FITC positive" than WT LCs, suggesting that they had spent longer in the skin before reaching LNs. Furthermore, there was also a significantly reduced accumulation of $FITC^+$ migratory DCs (confirmed using CD103 staining[36]; data not shown) in D6-deficient, compared with WT, LNs (supplemental Figure 4C left panel). Importantly, no differences were seen in levels of $FITC^+$ resident LN DCs (supplemental Figure 4C right panel). Finally, we also confirmed impaired antigen presentation by subcutaneously administered OVA-loaded DCs in inflamed D6-deficient mice. Recall responses, measured by IFN-γ production after OVA restimulation, revealed lower antigen-specific T-cell responses in inflamed D6-deficient, than inflamed WT, mice (supplemental Figure 4D).

To examine the importance of inflammation for the differences seen in Figure 5A, we assessed LC migration in WT and D6-deficient mice that had not been previously inflamed. Although D6-deficient mice still displayed reduced accumulation of $FITC^+$ LCs in LNs, this was markedly less than that seen from inflamed skin (Figure 5D). Importantly, FITC itself is pro-inflammatory and so may have contributed to the slight reduction in $FITC^+$ LC migration to D6-deficient LNs. Overall, these data suggest that deficiencies in LC migration in D6-deficient mice are associated with an active inflammatory response.

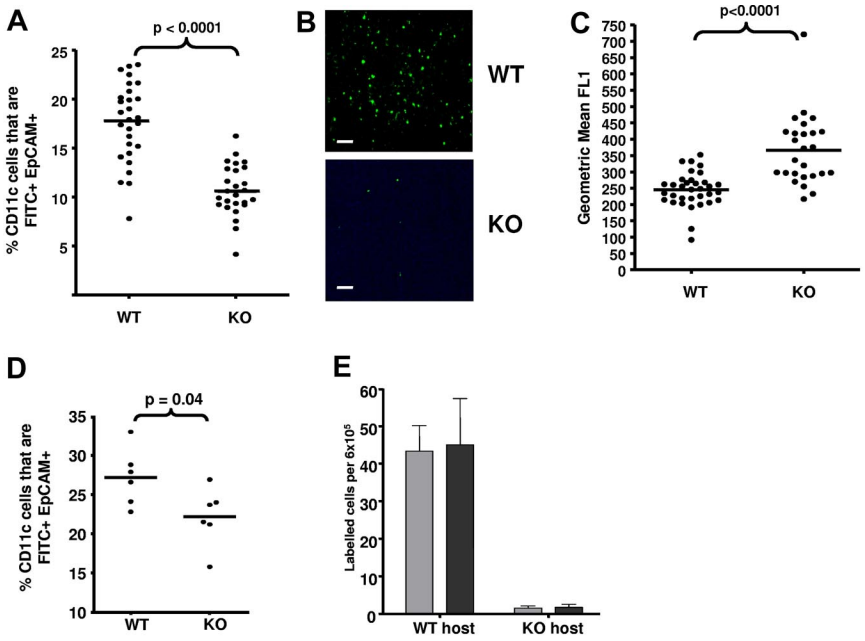

Figure 5. Impaired APC movement in inflamed D6-deficient mice. (A) D6-deficient mice show impaired LC trafficking from inflamed skin to LNs. The percentage of LN CD11c$^+$ cells that were FITC$^+$EpCAM$^+$ LC in LNs draining TPA-inflamed skin, 24 hours after FITC application, was assessed by flow cytometry. (B) Representative microscopic images of draining LNs, showing the differential presence of FITC (green)–positive leukocytes in WT and D6-deficient mice. Images were acquired at ×20 magnification on a Plan-Neoplmar 20×/0.5 objective. Scale bar represents 50 μm. (C) FITC intensity (mean fluorescence intensity) of LCs in draining LNs as measured by flow cytometry. (D) Inflammation is required for the impairment of LC migration to LNs in D6-deficient mice. FITC was applied to WT and D6-deficient mouse skin without prior inflammation and FITC$^+$EpCAM$^+$ LC numbers, in LNs, measured by flow cytometry. (E) Numbers of donor WT (gray) and D6-deficient (black) DCs present in draining LNs of inflamed host as determined by flow cytometry. Data are from 3 (A-C,E) and 2 (D) independent experiments with n > 3 mice per experimental group for each individual experiment.

We have reported that D6 is expressed on BMDCs,[21] and so we differentially labeled WT and D6-deficient BMDCs to separately examine their migration to LNs. In inflamed WT hosts (Figure 5E), considerable and comparable migration of BMDCs of both genotypes was detected in LNs. However, in inflamed D6-deficient mice, few labeled BMDCs of either genotype migrated to the draining LN. The lack of difference in migration of WT or D6-deficient BMDCs in either host indicates that D6 on DCs does not contribute to this phenomenon and that the absence of LEC D6 explains the defects in cell-trafficking from peripheral inflamed sites. This conclusion is also supported by radiation-chimera experiments (supplemental Figure 5), showing impaired dermal DC migration only in mice with D6-deficient lymphatic vasculature (WT into KO).

Together, these data indicate that fluid, cellular flow and antigen presentation from peripheral inflamed tissues to draining LNs are impaired in inflamed D6-deficient mice and that this is an LEC-specific phenomenon.

CCL2/CCR2 regulate lymphatic vessel congestion in D6-deficient mice

LECs, in inflamed conditions, express CCL2[37,38] (and Figure 1C). We therefore examined involvement of CCL2 and its receptor, CCR2, in myelomonocytic cell accumulation in draining LNs of D6-deficient mice. Immunohistochemical analysis of popliteal LNs, draining LPS-injected footpads, revealed CCL2 on Lyve1$^+$ lymphatic endothelium in the subcapsular sinus area (Figure 6A). In addition, using AlexaFluor(AF)–labeled CCL2, and flow cytometry, we have shown that CD11b$^+$Gr1^{low} cells expressed low levels and CD11b$^+$Gr1^{hi} cells expressed high levels of CCR2 (Figure 6B), suggesting that CCL2 and CCR2 may contribute to the inappropriate subcapsular accumulation of CD11b$^+$Gr1$^+$ cells in LNs of D6-deficient mice. To test this, we used a CCR2 antagonist (RS-504393[39]), in the context of LPS-induced footpad inflammation, to show that blocking CCR2 prevents myelomonocytic cell accumulation in D6-deficient popliteal LN draining the inflamed site (Figure 6C). This is seen for both CD11b$^+$Gr1^{low} and CD11b$^+$Gr1^{hi} cells but, in keeping with their higher CCR2 levels, is more complete for CD11b$^+$Gr1^{hi} cells. To test whether this also released lymphatic congestion and reestablished efficient antigen presentation, we performed FITC-painting experiments in D6-deficient mice treated with the CCR2 blocker. Blockage of CCR2 significantly reestablished LC migration to draining LNs in inflamed D6-deficient mice, confirming a role for CCR2 in the block in cellular trafficking from inflamed skin to LNs (Figure 6D). In addition, in vivo imaging system imaging of subcutaneously injected fluorescent-BSA revealed that blocking CCR2 also reversed the impaired fluid flow from inflamed sites to LNs in D6-deficient mice (data not shown). Interestingly, the effects of the CCR2 blocker in Figure 6D are incomplete, suggesting involvement of other inflammatory CC-chemokines in the impaired LC migration. Thus, CCL2/CCR2 interactions account for impaired lymphatic function, and reduced APC migration, in D6-deficient mice.

A model for D6 regulation of lymphatic function

The data in Figure 6 show that D6 prevents association of inflammatory CC-chemokines, especially CCL2, with LEC surfaces. Therefore, in WT mice, inflammatory CC-chemokines adhering to LEC surfaces will be removed through D6-dependent scavenging, but those adhering to D6-deficient LECs will not. One possible consequence of this (Figure 6E) is that, in contrast to WT LEC surfaces, inflammatory chemokine receptor-expressing cells may be able to interact, via chemokine/receptor/integrin-mediated attachments, to surface-presented inflammatory CC-chemokines on D6-deficient LECs. To test this, and given the difficulties in transfecting and working with LECs in vitro, we used HUVECs as a model of inflammatory leukocyte binding to endothelial cells.[40] In this model, HUVECs are treated with TNF to induce inflammatory CC-chemokines (including CCL2), selectins, and intergrins. These are presented on the HUVEC surface allowing attachment of THP-1 or other inflammatory chemokine receptor-bearing cells.[41,42] We performed this experiment using control HUVECs (which are D6-negative) and transfected HUVECs expressing D6-GFP. As

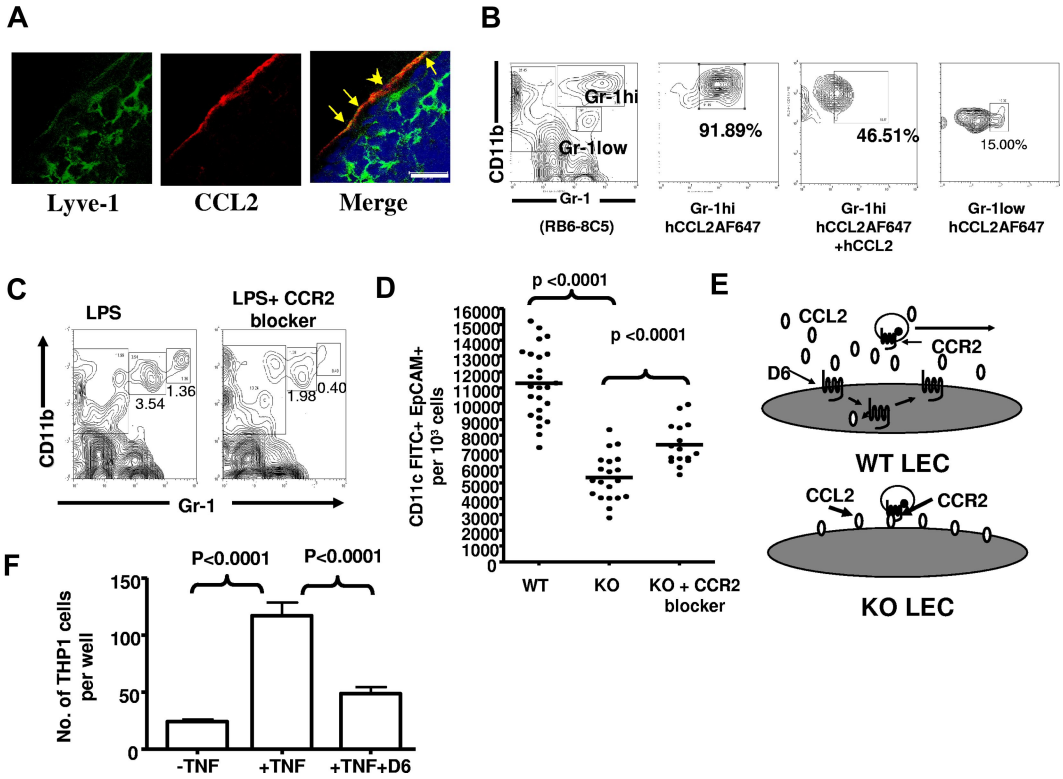

Figure 6. CCL2/CCR2 dependence of perilymphatic cellular accumulation in D6-deficient mice. (A) Confocal images representing the localization of CCL2 (red) on Lyve1$^+$ lymphatic vessels (green) surrounding the subcapsular sinus of a popliteal LN of a D6-deficient mouse 24 hours after subcutaneously footpad injection of LPS. DAPI (blue) was used for nuclear staining (blue). LECs showing Lyve1 and CCR2 positivity are marked by yellow arrows. Images were acquired at ×63 magnification with a scan zoom at 2.0 on a Plan-Apochromat 63×/1.4 oil Ph3 objective. Scale bar represents 20 μm. (B) CD11b$^+$Gr1^{hi} cells express CCR2. Popliteal LN cells collected from D6-deficient mice, 24 hours after footpad LPS injection, were incubated with AF-647–labeled human (h) CCL2, in the presence or absence of a 10-fold molar excess of unlabeled hCCL2 at 37°C for 30 minutes, and analyzed by flow cytometry. The data show CCL2 binding by CD11b$^+$Gr1^{hi} but less by CD11b$^+$Gr1^{low} cells. Cells that were left unstained were used as a control for background fluorescence. (C) CCR2 is involved in the accumulation of myelomonocytic cells in D6-deficient LNs. Two representative contour plots showing the ability of a CCR2 blocker (RS504393) to reduce numbers of CD11b$^+$Gr1$^+$ cells in D6-deficient politeal LNs 2 hours after subcutaneously footpad administration of LPS. (D) Intravenous administration of a CCR2 antagonist partially restored LC (CD11c$^+$EpCAM$^+$FITC$^+$) migration from inflamed skin to draining LNs in D6-deficient mice. (E) A diagrammatic representation of the hypothesized role for D6 on LECs. (F) D6 impairs inflammatory leukocyte binding to HUVECs. Control HUVECs or HUVECs transfected with D6-GFP were activated by TNF and TAMRA-labeled THP-1 cell binding measured. Data are from 3 (C) and 2 (A-B,D,F) independent experiments with n > 3 mice per experimental group for each individual experiments.

shown in Figure 6F, TNF treatment enhanced THP-1 binding to HUVECs, and this was suppressed by D6 expression in the HUVECs, supporting the model in Figure 6E.

Thus, these data demonstrate that D6, on a cell-autonomous basis, can prevent CC-chemokine–dependent association of inflammatory leukocytes with endothelial cells and provides a mechanistic explanation for the lymphatic congestion and CCL2-dependent, LEC-associated, myelomonocytic cellular accumulation apparent in inflamed D6-deficient mice.

Discussion

Previous studies of D6 have focused on its involvement in resolution of inflammatory responses.[5,6] However, a number of observations suggest that this may not be its sole, or even primary, function. For example, analysis of D6-expressing cells failed to identify a suitable vehicle for localized-scavenging of chemokines required for resolution of tissue inflammatory responses.[19-21] In addition, we have reported reduced response of D6-deficient mice in a model of autoimmune CNS disease,[33] indicating that D6 is not always anti–inflammatory. Here we have analyzed D6 in further detail and reveal a hitherto unanticipated in vivo role for D6 at inflamed lymphatic endothelial surfaces. Specifically, we have identified D6 as being essential for ensuring efficient flow of fluid and cells from peripheral inflamed sites to local draining LNs as well as the flow of inflammatory leukocytes within lymph. In the absence of D6, inappropriate presentation of inflammatory CC-chemokines on lymphatic endothelial surfaces results in perilymphatic accumulation of inflammatory leukocytes at peripheral inflamed sites. In addition, inflammatory chemokine presentation on subcapsular LECs within LNs "locks down" myelomonocytic cells, normally transiting in lymph, further contributing to lymphatic congestion. The consequences of this are that fluid flow and movement of APCs from inflamed tissues to draining LNs are impaired in D6-deficient mice. It is important to note that, although most of our data relate to CCL2, the ability of D6 to scavenge all inflammatory CC-chemokines suggests that it will maintain LEC surfaces free of each of these molecules. Together, our data suggest that D6 plays a fundamental role in ensuring efficiency of lymphatic drainage and antigen presentation in inflamed peripheral contexts. Furthermore, the data suggest that the inability of D6-deficient mice to resolve inflammatory responses may be an indirect consequence of impaired fluid, chemokine and cell drainage from inflamed peripheral sites and not a result of an inability to scavenge chemokines at inflamed sites as originally postulated.

We are aware of the apparent contradiction between impaired lymph flow and cellular accumulation in draining LNs. We account

for this on the basis of myelomonocytic cells "locking onto" lymphatic surfaces in both peripheral tissues and LNs, thus preventing lymph flow. We hypothesize that accumulation of the $CD11b^+Gr1^+$ cells (present in lymph) in LNs leads to exaggerated leukocyte recruitment, through HEVs, thus accounting for the increased LN size in the absence of free lymph flow. This is akin to previously reported effects of small numbers of DCs on LN size.[31]

Our data show that D6 does not block inflammatory CC-chemokine entry from inflamed sites to the lymphatic circulation. This agrees with previous studies demonstrating the ability of peripherally administered chemokines to enter LNs, in particular via the specialized conduit system.[43] Indeed, chemokines draining to LNs from inflamed sites may be important for coordinating peripheral inflammation with leukocyte recruitment through high endothelial venules. This is referred to as "remote control"[44] and has been specifically demonstrated for CCL2. In addition, LEC expression of CCL2 and other inflammatory chemokines during inflammation will also contribute to the lymph-borne presence of inflammatory CC-chemokines. Thus, inflammatory CC-chemokine movement from inflamed sites into lymph is normal, and even important, and probably accounts for much of the inflammatory chemokine presence in plasma of patients with inflammatory pathologies. In contrast, inflammatory CC-chemokine deposition on LECs is not normal and, we propose, is the basis for the phenotypes observed in the present study.

These insights into the in vivo function of D6 also help explain why CCR7 up-regulation is required for egress of APCs,[4] and other cells,[45] from peripheral tissues to LNs. Recent studies suggest that cellular egress to LNs requires LEC presentation of CCR7 ligands and possibly[38,46] integrin-mediated associations with lymphatic endothelium. Why cells cannot egress in response to inflammatory chemokines localized on lymphatic endothelial surfaces, or indeed produced by lymphatic endothelium,[47] has not so far been explained. In this context, we propose that D6, on LECs, scavenges inflammatory CC-chemokines on contact with lymphatic endothelium. This ensures that APCs, such as immature DCs, can enter a tissue and sample antigen without becoming adherent to lymphatic vessels through inappropriate interactions, with immobilized inflammatory CC-chemokines.

In conclusion, we demonstrate that D6 plays a fundamental role in regulating the efficiency of fluid, and cellular, trafficking from inflamed peripheral sites to LNs by ensuring that lymphatic surfaces are free of inflammatory leukocyte congestion. These data highlight D6 as a novel, LEC-expressed, in vivo coordinator of innate and adaptive immune responses.

Acknowledgments

This work was supported by the Wellcome Trust and Medical Research Council (G.J.G., R.J.N., and P.G.), Biotechnology and Biological Sciences Research Council (BBSRC, G.J.G. and R.J.N.), INNOCHEM EU (G.J.G.), and the National MS Society (grant RG3980, R.R. and L.P.L.).

Authorship

Contribution: K.M.L., C.S.M., D.S.G., K.J.P., V.M., C.J., L.P.L., S.M., and V.C. performed experiments; G.J.G., R.J.N., R.R., and P.G. designed experiments; and K.M.L., C.S.M., and G.J.G. wrote the paper.

Conflict-of-interest disclosure: The authors declare no competing financial interests.

Correspondence: Gerard J. Graham, Division of Immunology, Infection and Inflammation, Glasgow Biomedical Research Centre, University of Glasgow, 120 University Place, Glasgow, G128TA, United Kingdom; e-mail: g.graham@clinmed.gla.ac.uk.

References

1. Witte MH, Jones K, Wilting J, et al. Structure function relationships in the lymphatic system and implications for cancer biology. *Cancer Metastasis Rev*. 2006;25(2):159-184.
2. Rot A, von Andrian UH. Chemokines in innate and adaptive host defense: basic chemokinese grammar for immune cells. *Annu Rev Immunol*. 2004;22:891-928.
3. Mantovani A. The chemokine system: redundancy for robust outputs. *Immunol Today*. 1999; 20(6):254-257.
4. Forster R, Davalos-Misslitz AC, Rot A. CCR7 and its ligands: balancing immunity and tolerance. *Nat Rev Immunol*. 2008;8(5):362-371.
5. Graham GJ. D6 and the atypical chemokine receptor family: novel regulators of immune and inflammatory processes. *Eur J Immunol*. 2009; 39(2):342-351.
6. Mantovani A, Bonecchi R, Locati M. Tuning inflammation and immunity by chemokine sequestration: decoys and more. *Nat Rev Immunol*. 2006;6(12):907-918.
7. Boidajipour B, Mahabaleshwar H, Kardash E, et al. Control of chemokine-guided cell migration by ligand sequestration. *Cell*. 2008;132(3):463-473.
8. Fra AM, Locati M, Otero K, et al. Cutting edge: scavenging of inflammatory CC chemokines by the promiscuous putatively silent chemokine receptor D6. *J Immunol*. 2003;170(5):2279-2282.
9. Weber M, Blair E, Simpson CV, et al. The chemokine receptor D6 constitutively traffics to and from the cell surface to internalize and degrade chemokines. *Mol Biol Cell*. 2004;15(5):2492-2508.
10. Nibbs RJ, Wylie SM, Yang J, Landau NR, Graham GJ. Cloning and characterization of a novel promiscuous human beta-chemokine receptor D6. *J Biol Chem*. 1997;272(51):32078-32083.
11. Bonecchi R, Locati M, Galliera E, et al. Differential recognition and scavenging of native and truncated macrophage-derived chemokine (macrophage-derived chemokine/CC chemokine ligand 22) by the D6 decoy receptor. *J Immunol*. 2004;172(8):4972-4976.
12. Nibbs RJ, Wylie SM, Pragnell IB, Graham GJ. Cloning and characterization of a novel murine beta chemokine receptor, D6: comparison to three other related macrophage inflammatory protein-1alpha receptors, CCR-1, CCR-3, and CCR-5. *J Biol Chem*. 1997;272(19):12495-12504.
13. Di Liberto D, Locati M, Caccamo N, et al. Role of the chemokine decoy receptor D6 in balancing inflammation, immune activation, and antimicrobial resistance in Mycobacterium tuberculosis infection. *J Exp Med*. 2008;205(9):2075-2084.
14. Jamieson T, Cook DN, Nibbs RJ, et al. The chemokine receptor D6 limits the inflammatory response in vivo. *Nat Immunol*. 2005;6(4):403-411.
15. Martinez de la Torre Y, Buracchi C, Borroni EM, et al. Protection against inflammation- and autoantibody-caused fetal loss by the chemokine decoy receptor D6. *Proc Natl Acad Sci U S A*. 2007; 104(7):2319-2324.
16. Martinez de la Torre Y, Locati M, Buracchi C, et al. Increased inflammation in mice deficient for the chemokine decoy receptor D6. *Eur J Immunol*. 2005;35(5):1342-1346.
17. Vetrano S, Borroni EM, Sarukhan A, et al. The lymphatic system controls intestinal inflammation and inflammation-associated colon cancer through the chemokine decoy receptor D6. *Gut* 2010;59(2):197-206.
18. Whitehead GS, Wang T, DeGraff LM, et al. The chemokine receptor D6 has opposing effects on allergic inflammation and airway reactivity. *Am J Respir Crit Care Med*. 2007;175(3):243-249.
19. Nibbs RJ, Kriehuber E, Ponath PD, et al. The beta-chemokine receptor D6 is expressed by lymphatic endothelium and a subset of vascular tumors. *Am J Pathol*. 2001;158(3):867-877.
20. Graham GJ, McKimmie CS. Chemokine scavenging by D6: a movable feast? *Trends Immunol*. 2006;27(8):381-386.
21. McKimmie CS, Fraser AR, Hansell C, et al. Hemopoietic cell expression of the chemokine decoy receptor D6 is dynamic and regulated by GATA1. *J Immunol*. 2008;181(5):3353-3363.
22. Nibbs RJ, Gilchrist DS, King V, et al. The atypical chemokine receptor D6 suppresses the development of chemically induced skin tumors. *J Clin Invest*. 2007;117(7):1884-1892.
23. Milling SW, Jenkins C, MacPherson G. Collection of lymph-borne dendritic cells in the rat. *Nat Protoc*. 2006;1(5):2263-2270.

24. Edwards JC, Sedgwick AD, Willoughby DA. The formation of a structure with the features of synovial lining by subcutaneous injection of air: an in vivo tissue culture system. *J Pathol*. 1981;134(2):147-156.
25. Nibbs RJ, Yang J, Landau NR, Mao JH, Graham GJ. LD78beta, a non-allelic variant of human MIP-1alpha (LD78alpha), has enhanced receptor interactions and potent HIV suppressive activity. *J Biol Chem*. 1999;274(25):17478-17483.
26. Forster R, Schubel A, Breitfeld D, et al. CCR7 coordinates the primary immune response by establishing functional microenvironments in secondary lymphoid organs. *Cell*. 1999;99(1):23-33.
27. Xu Y, Zhan Y, Lew AM, Naik SH, Kershaw MH. Differential development of murine dendritic cells by GM-CSF versus Flt3 ligand has implications for inflammation and trafficking. *J Immunol*. 2007;179(11):7577-7584.
28. McKimmie CS, Moore M, Fraser AR, et al. A TLR2 ligand suppresses inflammation by modulation of chemokine receptors and redirection of leukocyte migration. *Blood*. 2009;113(18):4224-4231.
29. Hernandez-Hoyos G, Joseph S, Miller NG, Butcher GW. The lymphopenia mutation of the BB rat causes inappropriate apoptosis of mature thymocytes. *Eur J Immunol*. 1999;29(6):1832-1841.
30. Itano AA, McSorley SJ, Reinhardt RL, et al. Distinct dendritic cell populations sequentially present antigen to CD4 T cells and stimulate different aspects of cell-mediated immunity. *Immunity*. 2003;19(1):47-57.
31. MartIn-Fontecha A, Sebastiani S, Hopken UE, et al. Regulation of dendritic cell migration to the draining lymph node: impact on T lymphocyte traffic and priming. *J Exp Med*. 2003;198(4):615-621.
32. Milling S, Yrlid U, Cerovic V, MacPherson G. Subsets of migrating intestinal dendritic cells. *Immunol Rev*; 2010;234(1):259-267.
33. Liu L, Graham GJ, Damodaran A, et al. Cutting edge: the silent chemokine receptor d6 is required for generating T cell responses that mediate experimental autoimmune encephalomyelitis. *J Immunol*. 2006;177(1):17-21.
34. Nagao K, Ginhoux F, Leitner WW, et al. Murine epidermal Langerhans cells and langerin-expressing dermal dendritic cells are unrelated and exhibit distinct functions. *Proc Natl Acad Sci U S A*. 2009;106(9):3312-3317.
35. Britschgi MR, Favre S, Luther SA. CCL21 is sufficient to mediate DC migration, maturation and function in the absence of CCL19. *Eur J Immunol* 2010;40(5):1266-1271.
36. Bedoui S, Whitney PG, Waithman J, et al. Cross-presentation of viral and self antigens by skin-derived CD103+ dendritic cells. *Nat Immunol*. 2009;10(5):488-495.
37. Sironi M, Conti A, Bernasconi S, et al. Generation and characterization of a mouse lymphatic endothelial cell line. *Cell Tissue Res*. 2006;325(1):91-100.
38. Johnson LA, Clasper S, Holt AP, Lalor PF, Baban D, Jackson DG. An inflammation-induced mechanism for leukocyte transmigration across lymphatic vessel endothelium. *J Exp Med*. 2006;203(12):2763-2777.
39. Mirzadegan T, Diehl F, Ebi B, et al. Identification of the binding site for a novel class of CCR2b chemokine receptor antagonists: binding to a common chemokine receptor motif within the helical bundle. *J Biol Chem*. 2000;275(33):25562-25571.
40. Thomas-Ecker S, Lindecke A, Hatzmann W, Kaltschmidt C, Zanker KS, Dittmar T. Alteration in the gene expression pattern of primary monocytes after adhesion to endothelial cells. *Proc Natl Acad Sci U S A*. 2007;104(13):5539-5544.
41. Mackay F, Loetscher H, Stueber D, Gehr G, Lesslauer W. Tumor necrosis factor alpha (TNF-alpha)-induced cell adhesion to human endothelial cells is under dominant control of one TNF receptor type, TNF-R55. *J Exp Med*. 1993;177(5):1277-1286.
42. Viemann D, Goebeler M, Schmid S, et al. TNF induces distinct gene expression programs in microvascular and macrovascular human endothelial cells. *J Leukoc Biol*. 2006;80(1):174-185.
43. Gretz JE, Norbury CC, Anderson AO, Proudfoot AE, Shaw S. Lymph-borne chemokines and other low molecular weight molecules reach high endothelial venules via specialized conduits while a functional barrier limits access to the lymphocyte microenvironments in lymph node cortex. *J Exp Med*. 2000;192(10):1425-1440.
44. Palframan RT, Jung S, Cheng G, et al. Inflammatory chemokine transport and presentation in HEV: a remote control mechanism for monocyte recruitment to lymph nodes in inflamed tissues. *J Exp Med*. 2001;194(9):1361-1373.
45. Bromley SK, Thomas SY, Luster AD. Chemokine receptor CCR7 guides T cell exit from peripheral tissues and entry into afferent lymphatics. *Nat Immunol*. 2005;6(9):895-901.
46. Pflicke H, Sixt M. Preformed portals facilitate dendritic cell entry into afferent lymphatic vessels. *J Exp Med*. 2009;206(13):2925-2235.
47. Mancardi S, Vecile E, Dusetti N, et al. Evidence of CXC, CC and C chemokine production by lymphatic endothelial cells. *Immunology*. 2003;108(4):523-530.